Published in final edited form as:
J Phys Chem B. 2010 July 1; 114(25): 8425–8430. doi:10.1021/jp100765v.

Exploring Solvent Effects upon the Menshutkin Reaction using a Polarizable Force Field

Orlando Acevedo[†,*] and **William L. Jorgensen**[‡]

[†]Department of Chemistry and Biochemistry, Auburn University, Auburn, Alabama 36849

[‡]Department of Chemistry, Yale University, 225 Prospect Street, New Haven, Connecticut 06520-8107

Abstract

The energetics of the Menshutkin reaction between triethylamine and ethyl iodide have been computed using B3LYP and MP2 with the LANL2DZ, LANL2DZd, SVP, MIDI!, 6–311G(d,p), and aug-cc-PVTZ basis sets. Small- and large-core energy-consistent relativistic pseudopotentials were employed. Solvent effect corrections were computed from QM/MM Monte Carlo simulations utilizing free-energy perturbation theory, PDDG/PM3, and both a non-polarizable OPLS and polarizable OPLS-AAP force field. The B3LYP/MIDI! theory level provided the best $\Delta G^{\ddagger}$ values with a mean absolute error (MAE) of 4.9 kcal/mol from experiment in cyclohexane, CCl_4, THF, DMSO, acetonitrile, water, and methanol. However, the relative rates in cyclohexane, and to a certain extent CCl_4, were determined to be greatly underestimated when using the non-polarizable OPLS force field. An overall reduction in the MAE to 3.1 kcal/mol using B3LYP/MIDI!/OPLS-AAP demonstrated the need for a fully polarizable force field when computing solvent effects for highly dipolar transition structures in low-dielectric media. The MAEs obtained with PDDG/PM3/OPLS and OPLS-AAP of 5.3 and 3.8 kcal/mol, respectively, provided comparable results to B3LYP at a fraction of the computational resources. The large rate accelerations observed in the reaction were correlated to an increased stabilization of the emerging charge separation at the transition state via favorable solute-solvent interactions.

Introduction

The Menshutkin reaction is regarded as an important example for studying solvent effects upon the rates of reactions; there have been numerous prior experimental[1] and theoretical investigations.[2] Of relevance to this work is kinetic data reported for the Menshutkin reaction between triethylamine and ethyl iodide (Scheme 1) in 39 solvents that covers a rate range of 10^5.[3] The solvent dependence of the rates as the reaction proceeds from uncharged reactants to ions is complex and does not simply show increases with increasing solvent polarity. In fact, the rates in methanol and THF are about the same and 100-times less than in DMSO. In order to elucidate these dramatic kinetic effects at the atomic level, calculations at the B3LYP and MP2 theory levels have been carried out using multiple basis sets and pseudopotentials, e.g., LANL2DZ, LANL2DZd, SVP, MIDI!, 6–311G(d,p), and aug-cc-PVTZ. Changes in solvation along the reaction path were fully characterized in three major classes of solvents: nonpolar aprotic (cyclohexane and CCl_4), dipolar aprotic (THF, DMSO, and acetonitrile), and polar

orlando.acevedo@auburn.edu.

Supporting Information Available: Additional solute-solvent energy pair distributions; energies, frequencies, and coordinates of structures computed using *ab initio* and DFT methods; and complete ref 12. This material is available free of charge via the Internet at http://pubs.acs.org.

protic (methanol and water), by utilizing QM/MM Monte Carlo simulations featuring the PDDG/PM3 semiempirical method and a non-polarizable OPLS force field. The Menshutkin reaction can also provide a dramatic illustration of the effect of solvent polarizability on the rates of reaction in low-dielectric media since the dipole moment for the transition state is ca. 7.0 D.[3] Thus, solute geometries and $\Delta G^{\ddagger}$ for the reactions were also computed using a polarizable OPLS-AAP version of cyclohexane, CCl_4 and THF. Comparison among theory levels to complementary experimental results is given and further insight into solvent effects on the reaction is provided.

Computational Methods

Mixed quantum and molecular mechanical (QM/MM) calculations, as implemented in BOSS 4.7,[4] were carried out with the reacting system treated using the PDDG/PM3 semiempirical molecular orbital method.5 PDDG/PM3 has been extensively tested for gas-phase structures and energetics, and has given excellent results in solution-phase QM/MM studies for a wide variety of organic and enzymatic reactions.6 The solvent molecules are represented with the TIP4P-Ew water model7 and the united-atom[8] and all-atom OPLS force field[9] for the non-aqueous solvents. The periodic and tetragonal systems consisted of the reactants, plus 395 non-aqueous solvent molecules or 740 molecules for water. Ewald summations were used in conjunction with TIP4P-Ew for the aqueous simulations. To locate the minima and maxima on the free-energy surfaces, two-dimensional free-energy maps were constructed for each reaction in solution using the lengths of the two transforming bonds, R_{CN} and R_{CI}, as the reaction coordinates (Figure 1). Free-energy perturbation (FEP) calculations were performed in conjunction with NPT Metropolis Monte Carlo (MC) simulations at 25 °C and 1 atm. The reactant state was defined by R_{CN} = 5.0 Å, and the free-energy surfaces were flat in this vicinity.

In the present QM/MM implementation, the solute's intramolecular energy is treated quantum mechanically using PDDG/PM3; computation of the QM energy and atomic charges is performed for each attempted move of the solute, which occurs every 100 configurations. For electrostatic contributions to the solute-solvent energy, CM3 charges were obtained for the solute using PDDG/PM3 calculations with a scaling factor of 1.14. This is augmented with standard Lennard-Jones interactions between solute and solvent atoms using OPLS parameters. This combination is appropriate for a PM3-based method as it minimizes errors in computed free energies of hydration.[10] Solute-solvent and solvent-solvent intermolecular cutoff distances of 12 Å were employed based on all heavy atoms of the solute, e.g., oxygens of water and methanol and the central carbon and sulfur atoms of acetonitrile and DMSO. If any distance is within the cutoff, the entire solute-solvent or solvent-solvent interaction was included. Quadratic feathering of the intermolecular interactions within 0.5 Å of the cutoff was applied to soften the discontinuity in energy. Total translations and rotations were sampled in ranges that led to overall acceptance rates of about 40% for new configurations. Multiple FEP windows were run simultaneously on a Linux cluster at Auburn University.

Density functional theory (DFT) and *ab initio* calculations using the B3LYP and MP2 methods, [11] respectively, with varying basis sets were also used to characterize the transition structures and ground states in vacuum using Gaussian 03.[12] The QM calculations were used for geometry optimizations and computations of vibrational frequencies, which confirmed all stationary points as either minima or transition structures and provided thermodynamic corrections. All DFT and *ab initio* calculations were carried out on computers located at the Alabama Supercomputer Center.

Results and Discussion

Structures

Changes in free energy were calculated by perturbing the distances between the reacting nitrogen and carbon atoms (R_{CN}) and carbon and iodine atoms (R_{CI}) of the triethylamine and ethyl iodide Menshutkin reaction (Figures 1 and 2). The initial ranges for R_{CN} and R_{CI} were 1.7 – 2.7 Å and 2.4 – 3.1 Å, respectively, with an increment of 0.05 Å. Each FEP calculation entailed 5 million configurations of equilibration followed by 10 million configurations of averaging. The transition state was readily located and its corresponding region on the free energy surface was recomputed using increments of 0.01 Å. This provided refined geometries (± 0.02 Å) for the reaction in seven solvents of varying polarity (Table 1). The simulations predicted earlier transition structures correlated to increasing solvent polarity. For example, the reaction in DMSO yielded considerably longer making/breaking R_{CN} and R_{CI} bond lengths of 2.80 and 2.40 Å compared to gas-phase values of 2.64 and 2.05 Å. The R_{CN} reaction coordinate was particularly sensitive to polarity as the polar aprotic and protic solvents predicted considerably earlier transition structures compared to the lowest dielectric media, i.e., CCl_4 and cyclohexane (Table 1). The addition of polarizability to the low-dielectric solvent models also yielded earlier transition states compared to the same non-polarizable solvents. For example, the non-polarizable OPLS-AA force field gave a reacting R_{CN} distance of 2.10 Å for both CCl_4 and cyclohexane, however, the inclusion of polarizability increased the distances to 2.23 and 2.28 Å, respectively. In addition, the polarizable THF model also gave an earlier R_{CN} transition structure distance of 2.36 Å compared to 2.25 Å for the non-polarizable version.

Energetics

Computing the activation barriers for the Menshutkin reaction required ca. 200 FEP simulations per free energy map, e.g., Figure 2. In addition, further FEP calculations were required to refine the transition structures. As a result, the number of single-point QM calculations necessary to compute the final $\Delta G^{\ddagger}$ was well over 50 million per solvent. Consequently, use of fast QM methods such as PDDG/PM3 is the only viable option to investigate these liquid-state simulations using the on-the-fly QM/MM/MC methodology. The computed activation barriers for the Menshutkin reaction in solution are summarized in Table 2. The agreement between the PDDG/PM3 results and experiment are generally good; however, the $\Delta G^{\ddagger}$ values were dramatically overestimated in non-polar solvents, e.g., computed $\Delta G^{\ddagger}$ of 41.2 kcal/mol in cyclohexane compared to the experimental 26.6 kcal/mol. [3] Error ranges in the calculated free-energy values are estimated to be 0.6 kcal/mol from fluctuations in the ΔG values for each FEP window using the batch means procedure with batch sizes of 0.5 million configurations.[4]

While the errors in the low-dielectric media were determined to be primarily a consequence of use of the non-polarizable force field (see “Polarization Effects” section below), it would be adventageous to incorporate *ab initio* and density functional theory (DFT) methods into the solution-phase calculations for further comparisons. However, for proper study of organic reactions it is imperative that extensive sampling of the reactants and solvent molecules be carried out to obtain configurationally averaged free-energy changes.[6] Without adequate sampling, *ab initio* QM/MM methods have been shown to give significantly varied reaction and activation energies on similar configurations.[13] Alternative approaches for computing solvent effects could include the use of a continuum solvent model[14] or a “QM + MM” method featuring a minimum-energy reaction-path from *ab initio* calculations in the gas phase followed by importance sampling or FEP calculations in an explicit solvent box. Neither alternative is ideal as previous studies utilizing continuum-based treatments have revealed deficiencies in predicting rate differences between protic and aprotic solvents[6] and the “QM + MM” approach

relies on gas-phase reaction-path geometries which differ substantially from structures in solution (Table 1). Additional computational models for studying solvent effects are available, including the empirical valence bond (EVB),[15] modern valence bond theory (MOVB) method, 16 and ONIOM method,17 which could potentially provide accurate energies. For example, prior work by Dillet et al. utilized a custom continuum model to study solvent effects on the Menshutkin reaction between ammonia and methyl chloride that provided results comparable to explicit solvent models.2h

The present QM/MM/FEP/MC calculations were used to obtain free energies of solvation, ΔG_{solv}, for the Menshutkin reaction in 7 different solvents by taking the difference in free-energy from a PDDG/PM3-based FEP/MC gas-phase simulation and the solution-phase energies computed in Table 2. Since the same computational approach is used for both the gas-phase and solvated simulations, most errors including any deficiencies in the PDDG/PM3 method are expected to largely cancel out. $\Delta G^{\ddagger}$ values computed from gas-phase B3LYP and MP2 theory levels (Tables 3 and 4) were then corrected using the corresponding ΔG_{solv} values. To properly treat the large number of electrons present in iodine with QM methods, different basis sets were tested including ones using frozen-core approximations and relativistic pseudopotentials. Gaussian 03 has built into the program multiple basis sets capable of treating iodine, and in the present study the LANL2DZ,18 SVP,19 and MIDI![20] basis sets were tested. In addition, the 6–311G(d,p),21 LANL2DZd,18 aug-cc-PVTZ-PP,22 and SDB-aug-cc-PVTZ23 basis sets for iodine were obtained from the Environmental Molecular Sciences Laboratory (EMSL) Basis Set Exchange Database.[24] The B3LYP, MP2, and PDDG/PM3 methods all predicted similar $\Delta G^{\ddagger}$ gas-phase values of ~ 35 – 40 kcal/mol for the reaction between triethylamine and ethyl iodide (Table 3). However, B3LYP using mixed basis sets of 6-31+G(d,p) and aug-cc-PVDZ for C, H, and N, and the small-core (PP) and large-core (SDB) energy consistent relativistic pseudopotentials[22,23] with aug-cc-PVTZ on I yielded higher $\Delta G^{\ddagger}$ values of ~ 40 – 45 kcal/mol for the gas-phase Menshutkin reaction (Table 4).

Polarization Effects

The strong ion-molecule interactions that develop at the charge-separated transition state of the Menshutkin reaction implies that a polarizable force field may be required for proper treatment of solvent effects, particularly in low-dielectric media.[25] Accordingly, inducible dipoles were added to the non-hydrogen atoms in THF, CCl_4, and cyclohexane in a similar fashion to our recent study on anion-phenol complexes.[26] Briefly, the electric field that determines the inducible dipoles is computed from the permanent charges using Eq. 1, and the polarization energy is given by Eq. 2. As the induced dipoles do not contribute to the electric field, an iterative solution for the dipoles in not required. The addition of induced dipoles to the all-atom OPLS force field yields OPLS-AAP. The same first-order polarization model has been used in earlier studies with good success.[25–27] Values of 1.0 and 1.5 $Å^3$ were used for the polarizabilities, α_i, on carbon and heteroatoms, respectively, for THF and CCl_4.[26] For cyclohexane, an inducible dipole on each carbon with polarizability $\alpha_C = \alpha(C_6H_{12})/6 = 2.39$ $Å^3$ has been shown to accurately reproduce the experimental reduction in the gauche-trans ΔG for 1,2-dichloroethane upon transfer from the gas phase to cyclohexane and in the ΔG of solvation of water in cyclohexane.[25] Consequently, this value of α_C was used in the OPLS-AAP cyclohexane simulation.

$$\vec{\mu}_i = \alpha_i \vec{E}_i^0 \quad (1)$$

$$E_{pol} = -\left(\frac{1}{2}\right)\sum_i \vec{\mu}_i \cdot \vec{E}_i^0 \quad (2)$$

The polarizable cyclohexane solvent model provided a dramatic effect on the $\Delta G^{\ddagger}$ with an approximate difference of 10 kcal/mol between the OPLS-AAP and OPLS-AA force fields (Tables 2 and 6). For example, B3LYP/LANL2DZ + OPLS-AAP gave a $\Delta G^{\ddagger}$ of 27.0 kcal/mol, which is in good agreement with the experimental value of 26.6 kcal/mol in cyclohexane; [3] the unpolarized OPLS-AA version yielded a $\Delta G^{\ddagger}$ of 37.2 kcal/mol. Solvent polarization of CCl_4 gave a more modest drop in ΔG_{solv} of ca. −2.3 kcal/mol compared to the non-polarized OPLS version. Higher barriers were predicted for THF compared to the non-polarized version, e.g. $\Delta G^{\ddagger}$ from PDDG/PM3 increased from 23.1 to 25.0 kcal/mol, when employing the polarizable force field.

Mean Absolute Error (MAE)

The $\Delta G^{\ddagger}$ MAEs are given in Tables 8 and 9 for the condensed-phase Menshutkin reactions at different theory levels. The OPLS MAEs were calculated using the non-polarizable solvent models exclusively; however, the OPLS-AAP MAEs substituted the polarized versions of cyclohexane, CCl_4, and THF in addition to the non-polarizable water, methanol, acetonitrile, and DMSO solvent models. The OPLS MAEs were approximately 2 kcal/mol higher than OPLS-AAP values regardless of the theory level employed (Table 8). The majority of the OPLS-AAP MAE enhancement came from the substantially improved activation energies when using the polarized-version of cyclohexane, although improvements in $\Delta G^{\ddagger}$ for CCl_4 also contributed. The best performing method was the B3LYP/MIDI!, which gave MAEs of 4.9 and 3.1 kcal/mol for the OPLS and OPLS-AAP, respectively (Table 8). However, the LANL2DZ and LANL2DZd basis sets with the B3LYP and MP2 methods also provided close experimental agreement. Notably, the PDDG/PM3/OPLSAAP gave a MAE, 3.8 kcal/mol, comparable to the best performing theory levels; it also outperformed the B3LYP/6-311G(d,p) and MP2/LANL2DZd using only a fraction of the computational resources. The use of mixed basis sets did not offer any advantages over the standard methods in terms of speed or accuracy (Table 9).

Solvent Effects

To elucidate the origin of the relative rate differences for the condensed-phase Menshutkin reactions, solute-solvent energy pair distributions were computed. Solute-solvent energy pair distributions record the average number of solvent molecules that interact with the solute and the energy associated with those interactions. The energies are obtained by analyzing the QM/MM//MC results in representative FEP windows near the transition structure and reactants. The results for the reaction between triethylamine and ethyl iodide are shown in Figure 3 for water and DMSO. The solute-solvent energy pair distributions in the remaining solvents, i.e., CH_3CN, THF, CH_3OH, CCl_4, and cyclohexane, are given in the Supporting Information as Figures S1–S5. Hydrogen bonding in water and ion-dipole electrostatic interactions in DMSO are reflected in the left-most region. The most favorable solute-solvent interactions energies are generally more attractive than −4 kcal/mol, while the large peaks near 0 kcal/mol result from the many distant solvent molecules in the outer shells.

In aqueous solution, hydrogen bonding is stronger for the transition state owing to the charge separation present as the ion products begin to emerge. Approximately four additional water molecules organize themselves in going from the reactants to transition state as quantified by integrating the corresponding solute-solvent bands. For example, integrating from −15.0 to a cutoff energy of −4.5 kcal/mol yields 4.6 and 1.1 water molecules interacting with the transition

structure and the reactants, respectively. If the integration is extended to −4.0 kcal/mol, the corresponding values are 4.9 and 1.2. Gao reported that increases in the strength and total number of hydrogen bonds are critical for the stabilization of the transition state and products for a similar Menshukin reaction, ammonia and methyl chloride, in water.[28] However, the stabilization gained in the present reaction from the favorable electrostatic interactions is partially offset by the entropy penalty paid for organizing a greater number of water molecules around the transition state. Dipolar aprotic solvents such as DMSO and CH_3CN are not capable of providing the same intensity of dipole-ion interactions compared to water's hydrogen bonding ability, and the non-polar solvents provide no highly favorable solute-solvent interactions (see Supporting Information Figures S1–S5). However, the reactants in DMSO and CH_3CN were not favorably stabilized, in turn raising the ground-state energy; this may contribute to the overall lower activation barriers in these solvents relative to water. For example, in DMSO and CH_3CN, the number of solute-solvent interactions at the reactants is 0.2 and 0.0, respectively, when integrated to −4.5 kcal/mol, and 0.5 and 0.1 when integrated to −4.0 kcal/mol.

Conclusion

A computational mechanistic investigation utilizing different DFT and *ab initio* theory levels was carried out for the condensed-phase Menshutkin reaction between triethylamine and ethyl iodide. Good success in reproducing the experimentally observed free-energies of activation in 7 solvents, i.e., cyclohexane, CCl_4, THF, DMSO, acetonitrile, water, and methanol, was achieved by applying solvent corrections, ΔG_{solv}, derived from PDDG/PM3/MM/FEP/MC simulations. Changes in solvation along the reaction path were fully characterized using both a non-polarizable OPLS and polarizable OPLS-AAP force field. The agreement between the B3LYP, MP2, and PDDG/PM3 methods and experiment is generally good; however, the $\Delta G^{\ddagger}$ values using the non-polarizable force field were greatly overestimated in the non-polar solvents, i.e., cyclohexane and CCl_4. The error was largely resolved by using the polarizable OPLS-AAP force field. For example, B3LYP/LANL2DZ with OPLS-AAP gave a $\Delta G^{\ddagger}$ in cyclohexane of 27.0 kcal/mol, which is in close agreement with the experimental value of 26.6 kcal/mol;[3] the unpolarized OPLS-AA version yielded a $\Delta G^{\ddagger}$ of 37.2 kcal/mol. The non-polarized $\Delta G^{\ddagger}$ MAEs were approximately 2 kcal/mol higher than the OPLS-AAP regardless of the theory level employed; this emphasizes the need for a polarizable force field when computing solvent effects for highly dipolar transition structures in low-dielectric media.[25] The reaction coordinate was particularly sensitive to polarity as the more polar aprotic and protic solvents predicted considerably earlier transition structures compared to the non-polar solvents. The present results confirm the general view that the origin of the rate accelerations observed in the Menshutkin reaction are correlated to the enhanced stabilization provided by favorable interactions between the solvents and the emerging charge separation at the transition state.

Supplementary Material

Refer to Web version on PubMed Central for supplementary material.

Acknowledgments

Gratitude is expressed to the National Science Foundation (CHE0446920), the National Institutes of Health (GM32136), Auburn University, and the Alabama Supercomputer Center for support of this research.

References

1. (a) Yau HM, Howe AG, Hook JM, Croft AK, Harper JB. Org. Biomol. Chem 2009;7:3572–3575. [PubMed: 19675914] (b) Stanger KJ, Lee J-J, Smith BD. J. Org. Chem 2007;72:9663–9668. [PubMed:

17979296] (c) Abboud JLM, Notario R, Bertran J, Sola M. Prog. Phys. Org. Chem 1993;19:1–182. (d) Haberfield P, Nudelman A, Bloom A, Romm R, Ginsberg H. J. Org. Chem 1971;36:1792–1795. (e) Reinheimer JD, Harley JD, Meyers WW. J. Org. Chem 1963;28:1575–1579.

2. (a) Komeiji Y, Mochizuki Y, Nakano T, Fedorov DG. THEOCHEM 2009;898:2–7.Yamamoto T. J. Chem. Phys 2008;129:244104/1–244104/15. [PubMed: 19123492] (b) Su P, Wu W, Kelly CP, Cramer CJ, Truhlar DG. J. Phys. Chem. A 2008;112:12761–12768. [PubMed: 18671376] (c) Su P, Ying F, Wu W, Hiberty PC, Shaik S. ChemPhysChem 2007;8:2603–2614. [PubMed: 18061916] (d) Higashi M, Hayashi S, Kato S. J. Chem. Phys 2007;126:144503/1–144503/10. [PubMed: 17444719] (e) Ruiz-Pernía J, Silla E, Tuñón I, Martí S, Moliner V. J. Phys. Chem. B 2004;108:8427–8433. (f) Ohmiya K, Kato S. J. Chem. Phys 2003;119:1601–1610. (g) Truong TN, Truong TT, Stefanovich EV. J. Chem. Phys 1997;107:1881–1889. (h) Dillet V, Rinaldi D, Bertrán J, Rivail J-L. J. Chem. Phys 1996;104:9437–9444.
3. Abraham MH, Grellier PL. J. Chem. Soc., Perkin Trans 2 1976;1976:1735–1741.
4. Jorgensen WL, Tirado-Rives J. J. Comput. Chem 2005;26:1689–1700. [PubMed: 16200637]
5. (a) Repasky MP, Chandrasekhar J, Jorgensen WL. J. Comput. Chem 2002;23:1601–1622. [PubMed: 12395428] (b) Tubert-Brohman I, Guimarães CRW, Repasky MP, Jorgensen WL. J. Comput. Chem 2003;25:138–150. [PubMed: 14635001] (c) Tubert-Brohman I, Guimarães CRW, Jorgensen WL. J. Chem. Theory Comput 2005;1:817–823. [PubMed: 19011692]
6. (a) Acevedo O, Jorgensen WL. Acc. Chem. Res 2010;43:142–151. [PubMed: 19728702] (b) Acevedo O, Armacost K. J. Am. Chem. Soc 2010;132:1966–1975. [PubMed: 20088521]
7. Horn HW, Swope WC, Pitera JW, Madura JD, Dick TJ, Hura GL, Head-Gordon T. J. Chem. Phys 2004;120:9665–9678. [PubMed: 15267980]
8. (a) Jorgensen WL, Briggs JM. Mol. Phys 1988;63:547–558.Jorgensen WL. J. Phys. Chem 1986;90:1276–1284. (b) Jorgensen WL, Briggs JM, Contreras ML. J. Phys. Chem 1990;94:1683–1686.
9. Jorgensen WL, Maxwell DS, Tirado-Rives J. J. Am. Chem. Soc 1996;118:11225–11236.
10. Blagović MU, Morales de Tirado P, Pearlman SA, Jorgensen WL. J. Comput. Chem 2004;25:1322–1332. [PubMed: 15185325]
11. (a) Becke AD. J. Chem. Phys 1993;98:5648–5652. (b) Lee C, Yang W, Parr RG. Phys. Rev 1988;37:785–789.
12. Frisch, MJ. Gaussian 03, Revision B.05. Pittsburgh PA: Gaussian, Inc.; 2003. [Full reference given in Supporting Info.]
13. Klähn M, Braun-Sand S, Rosta E, Warshel A. J. Phys. Chem. B 2005;109:15645–15650. [PubMed: 16852982]
14. Tomasi J, Mennucci B, Cammi R. Chem. Rev 2005;105:2999–3093. [PubMed: 16092826]
15. Kamerlin SCL, Haranczyk M, Warshel A. J. Phys. Chem. B 2009;113:1253–1272. [PubMed: 19055405]
16. Mo Y, Gao J. J. Phys. Chem. A 2000;104:3012–3020.
17. Vreven T, Morokuma K. Ann. Rep. Comput. Chem 2006;2:35–51.
18. (a) Wadt WR, Hay PJ. J. Chem. Phys 1985;82:284–298. (b) Hay PJ, Wadt WR. J. Chem. Phys 1985;82:299–310.
19. Schäfer A, Horn H, Ahlrichs R. J. Chem. Phys 1992;97:2571–2577.
20. Li J, Cramer CJ, Truhlar DG. Theor. Chem. Acc 1998;99:192–196.
21. Glukhovstev MN, Pross A, McGrath MP, Radom L. J. Phys. Chem. B 1995;103:1878–1885.
22. Peterson KA, Shepler BC, Figgen D, Stoll H. J. Phys. Chem. A 2006;110:13877–13883. [PubMed: 17181347]
23. Martin JML, Sundermann A. J. Chem. Phys 2001;114:3408–3420.
24. (a) Feller D. J. Comput. Chem 1996;17:1571–1586. (b) Schuchardt KL, Didier BT, Elsethagen T, Sun L, Gurumoorthi V, Chase J, Li J, Windus TL. J. Chem. Inf. Model 2007;47:1045–1052. [PubMed: 17428029]
25. Jorgensen WL, McDonald NA, Selmi M, Rablen PR. J. Am. Chem. Soc 1995;117:11809–11810.
26. Jorgensen WL, Jensen KP, Alexandrova AN. J. Chem. Theory Comput 2007;3:1987–1992.

27. (a) King G, Warshel A. J. Chem. Phys 1990;93:8682–8692. (b) Straatsma TP, McCammon JA. Chem. Phys. Lett 1991;177:433–440. (c) Gao J. J. Comput. Chem 1997;18:1061–1071.

28. (a) Gao J, Xia X. J. Am. Chem. Soc 1993;115:9667–9675. (b) Gao J. J. Am. Chem. Soc 1991;113:9667–9675.

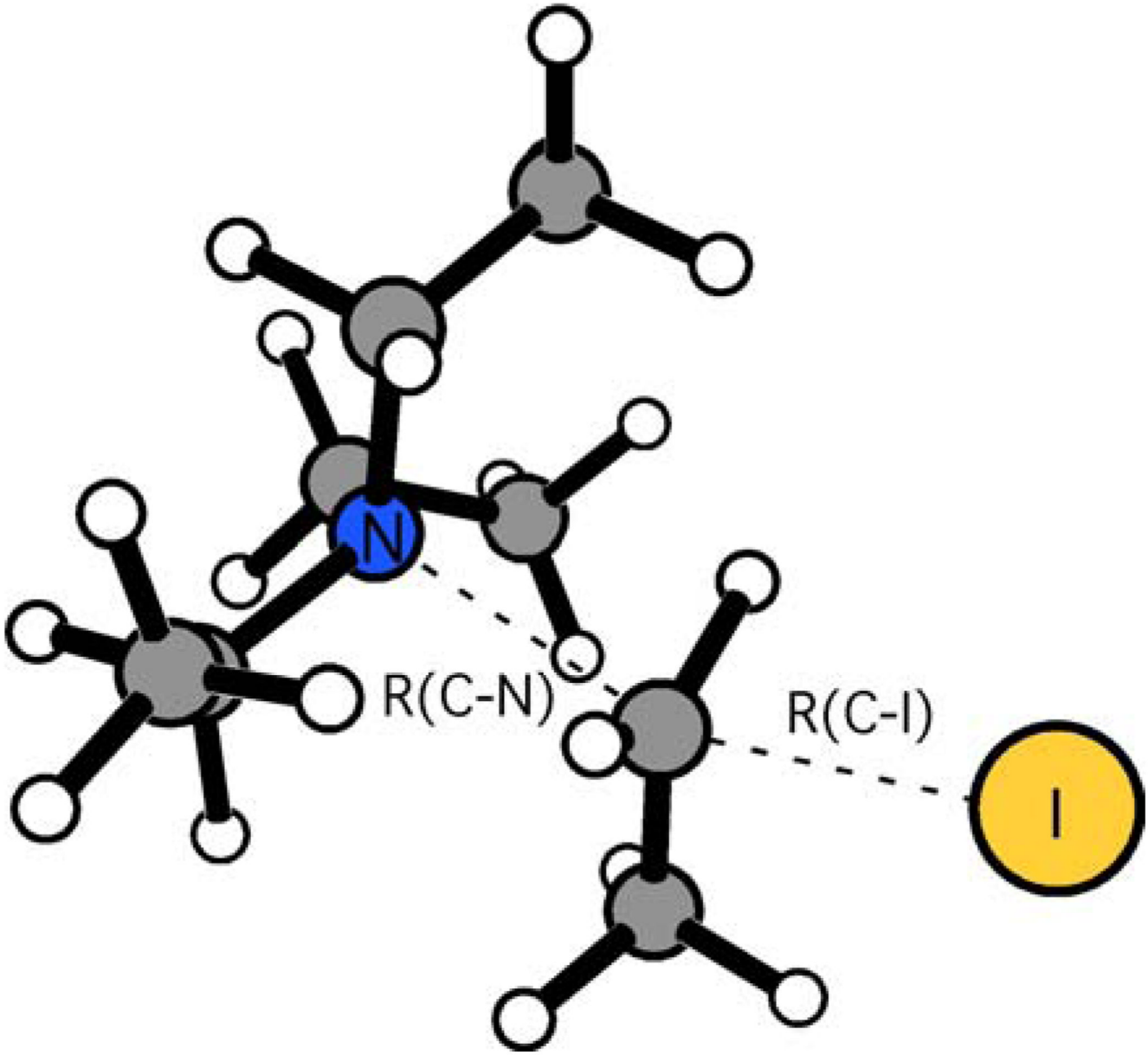

Figure 1.
Reaction coordinates, R_{CN} and R_{CI}, for the Menshutkin reaction between triethylamine and ethyl iodide. Illustrated structure is the transition structure from gas-phase PDDG/PM3 calculations.

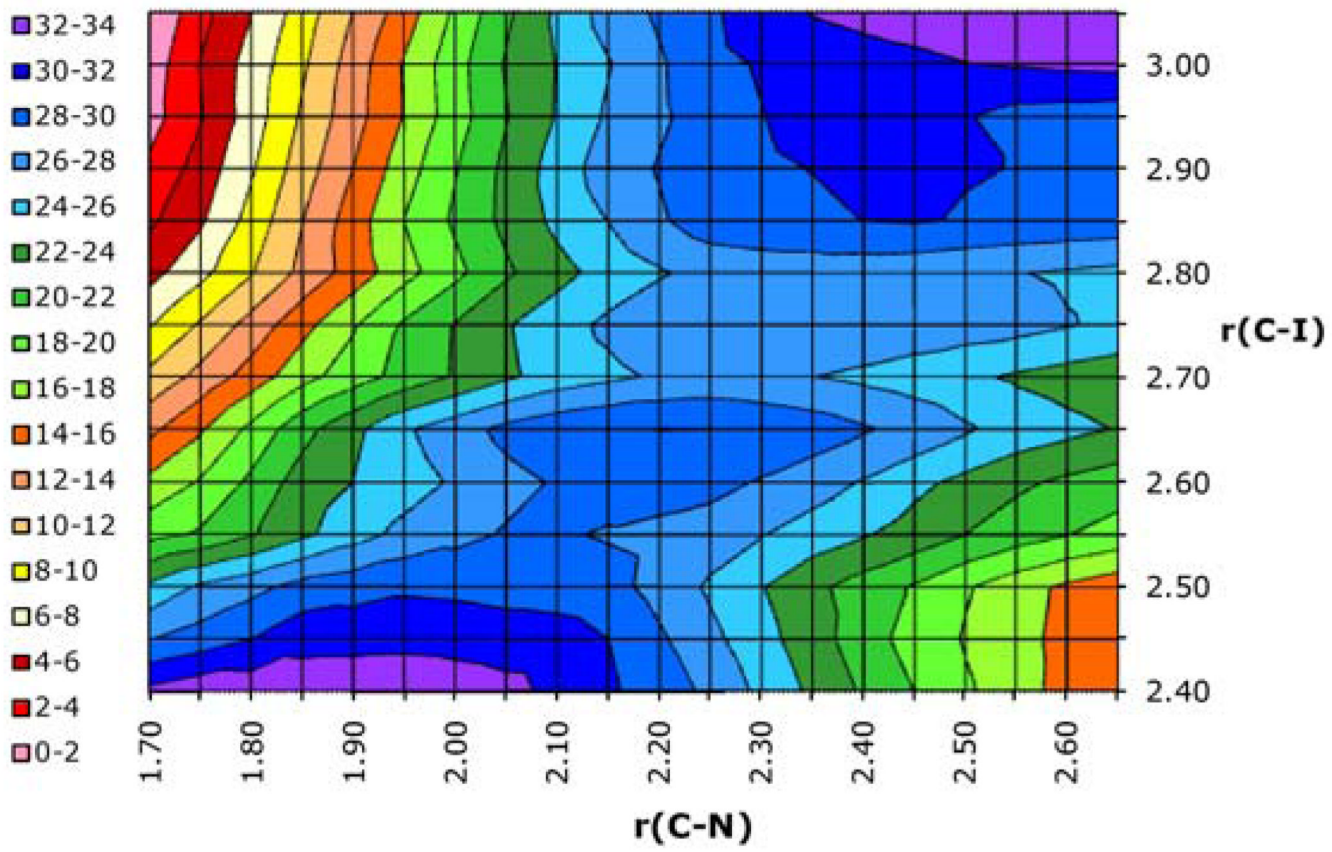

Figure 2.
Two-dimensional potential of mean force (free energy map; reaction coordinates R_{CN} and R_{CI}) for the Menshutkin reaction between triethylamine and ethyl iodide in cyclohexane using the polarizable OPLS-AAP force field. All distances in Å and energies in kcal/mol.

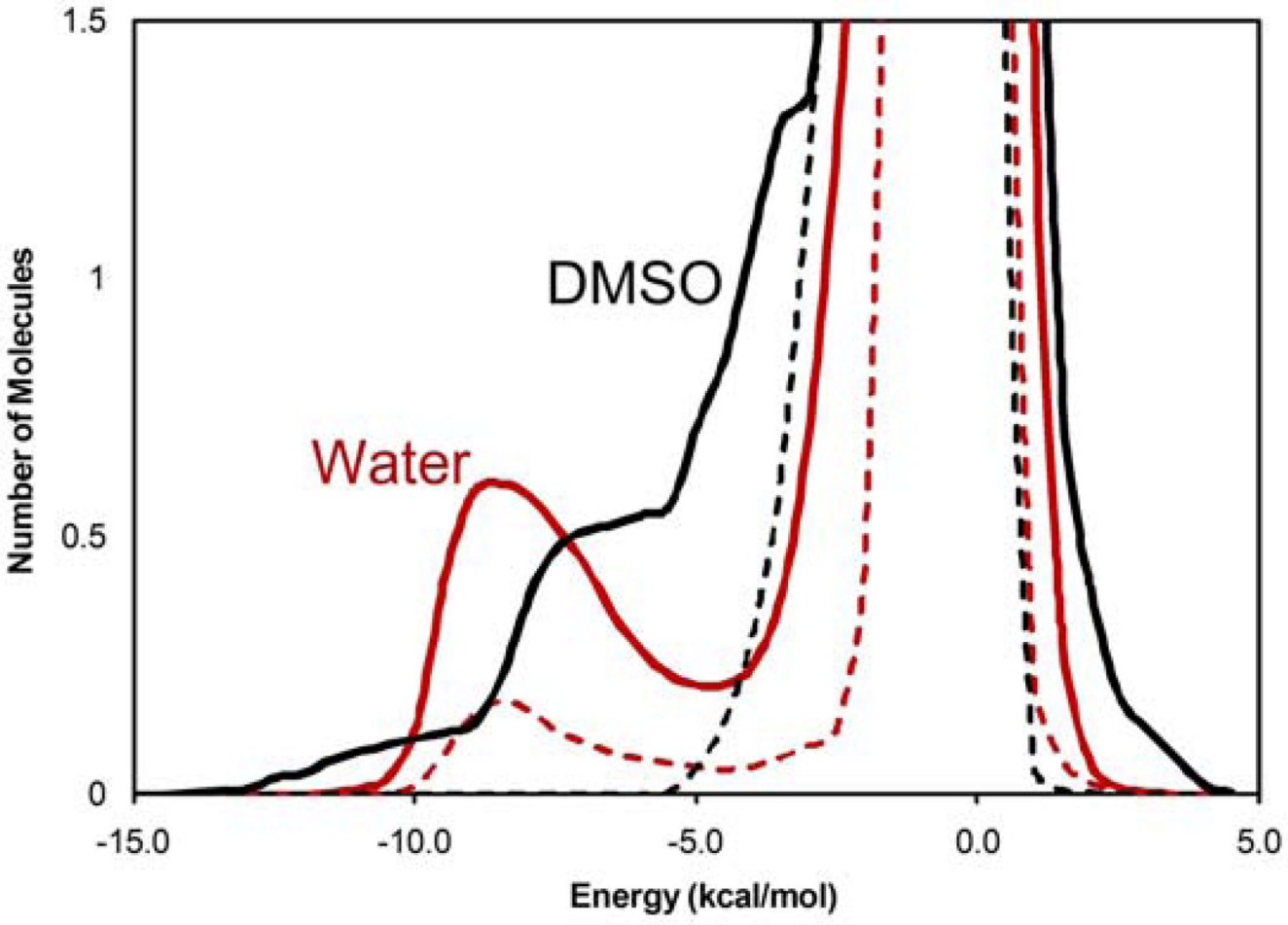

Figure 3.
Solute-solvent energy pair distributions at 25 °C for the Menshutkin reaction in water (red) and in DMSO (black). Results for the transition structures are represented by solid lines and for the reactants by dashed lines.

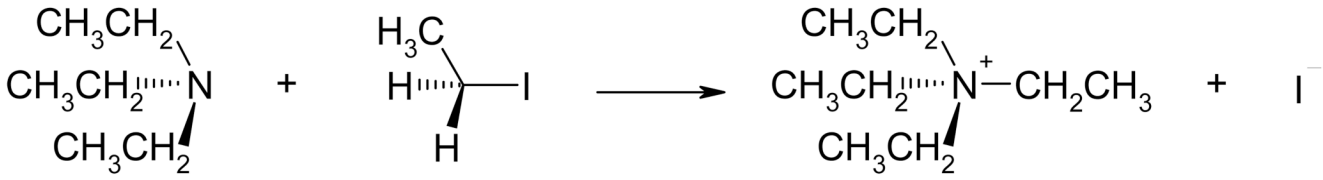

Scheme 1.
Menshutkin reaction between triethylamine and ethyl iodide.

Table 1

Computed Bond Lengths (Å) for the Transition Structures of the Menschutkin Reaction at 25 °C and 1 atm.[a]

	ε (D)	R_{CI}	R_{CN}
Gas	-	2.64	2.05
c-C_6H_{12}	2.02	2.70	2.10
c-C_6H_{12}-POL[b]	2.02	2.72	2.28
CCl_4	2.24	2.68	2.10
CCl_4-POL[b]	2.24	2.68	2.23
THF	7.58	2.71	2.25
THF-POL[b]	7.58	2.72	2.36
CH_3OH	32.7	2.71	2.55
CH_3CN	37.5	2.79	2.45
DMSO	46.7	2.80	2.40
Water	80.1	2.70	2.42

[a] From the 2D free-energy maps computed in the MC/FEP simulations and compared to experimental dielectric constants.

[b] Polarizable OPLS-AAP force field.

Table 2

Solution-Phase Free Energy Activation Barriers, $\Delta G^{\ddagger}$ (kcal/mol), for the Menshutkin Reaction Between Triethylamine and Ethyl Iodide.[a]

	DMSO	CH_3CN	Water	THF	CH_3OH	CCl_4	c-C_6H_{12}
B3LYP/LANL2DZ	17.3	17.1	20.5	19.0	14.7	33.1	37.2
B3LYP/LANL2DZd	17.8	17.6	21.0	19.5	15.2	33.6	37.7
B3LYP/SVP	24.6	24.4	27.8	26.3	22.0	40.4	44.5
B3LYP/MIDI!	20.1	19.9	23.3	21.8	17.5	35.9	40.0
B3LYP/6-311G(d,p)	22.1	21.9	25.3	23.8	19.5	37.9	42.0
MP2/LANL2DZ	17.5	17.3	20.7	19.2	14.9	33.3	37.4
MP2/LANL2DZd	13.6	13.4	16.8	15.3	11.0	29.4	33.5
PDDG/PM3	21.4	21.2	24.5	23.1	18.8	37.2	41.2
Experiment[b]	20.1	20.6	21.1	22.7	22.9	24.8	26.6

[a] Gas-phase QM results corrected for solvent effects using the PDDG/PM3-based FEP/MC simulations.

[b] Ref. 3.

Table 3

Gas-Phase Activation Barriers (kcal/mol) at 25 °C for the Menshutkin Reaction Between Triethylamine and Ethyl Iodide.

	$\Delta E^{\ddagger}_{0}$	$\Delta E^{\ddagger}$	$\Delta H^{\ddagger}$	$\Delta G^{\ddagger}$
B3LYP/LANL2DZ	23.0	23.4	22.8	35.3
B3LYP/LANL2DZd [a]	23.5	23.9	23.3	35.8
B3LYP/SVP	30.3	30.8	30.2	42.6
B3LYP/MIDI!	25.7	26.1	25.5	38.1
B3LYP/6-311G(d,p) [a]	28.0	28.4	27.9	40.1
MP2/LANL2DZ	22.7	22.9	22.3	35.5
MP2/LANL2DZd [a]	18.8	19.1	18.5	31.6
PDDG/PM3	-	-	-	39.4[b]

[a] Basis sets obtained from the EMSL basis set exchange.[24]

[b] MC/FEP result.

Table 4

Gas-Phase Activation Barriers (kcal/mol) at 25 °C for the Menshutkin Reaction Between Triethylamine and Ethyl Iodide Using B3LYP and Mixed Basis Sets.[a]

C, H, N	I	$\Delta E^{\ddagger}_{o}$	$\Delta E^{\ddagger}$	$\Delta H^{\ddagger}$	$\Delta G^{\ddagger}$
6-31+G(d,p)	aug-cc-PVTZ-PP	33.3	33.7	33.1	45.6
6-31+G(d,p)	SDB-aug-cc-PVTZ	33.1	33.5	32.9	45.4
aug-cc-PVDZ	aug-cc-PVTZ-PP	28.4	28.7	28.1	40.8
aug-cc-PVDZ	SDB-aug-cc-PVTZ	28.1	28.5	27.9	40.5

[a]Basis sets for I obtained from the EMSL basis set exchange.[24]

Table 5

Solution-Phase Free-Energy Activation Barriers, $\Delta G^{\ddagger}$ (kcal/mol), for the Menshutkin Reaction Between Triethylamine and Ethyl Iodide Using B3LYP and Mixed Basis Sets.[a]

C, H, N	I	DMSO	CH_3CN	Water	THF	CH_3OH	CCl_4	c-C_6H_{12}
6-31+G(d,p)	aug-cc-PVTZ-PP	27.6	27.4	30.8	29.3	25.0	43.4	47.5
6-31+G(d,p)	SDB-aug-cc-PVTZ	27.4	27.2	30.6	29.1	24.8	43.2	47.3
aug-cc-PVDZ	aug-cc-PVTZ-PP	22.8	22.6	26.0	24.5	20.2	38.6	42.7
aug-cc-PVDZ	SDB-aug-cc-PVTZ	22.5	22.3	25.7	24.2	19.9	38.3	42.4
	Experiment[b]	20.1	20.6	21.1	22.7	22.9	24.8	26.6

[a] Gas-phase QM calculations corrected for solvent effects using the PDDG/PM3-based MC/FEP simulations.

[b] Ref. 3.

Table 6

Solution-Phase Free Energy Activation Barriers, $\Delta G^{\ddagger}$ (kcal/mol), for the Menshutkin Reaction Between Triethylamine and Ethyl Iodide.[a]

	THF-POL	CCl_4-POL	c-C_6H_{12}-POL
B3LYP/LANL2DZ	20.9	30.8	27.0
B3LYP/LANL2DZd	21.4	31.3	27.5
B3LYP/SVP	28.2	38.1	34.3
B3LYP/MIDI!	23.7	33.6	29.8
B3LYP/6-311G(d,p)	25.7	35.6	31.8
MP2/LANL2DZ	21.1	31.0	27.2
MP2/LANL2DZd	17.2	27.1	23.3
PDDG/PM3	25.0	34.9	31.1
Experiment[b]	22.7	24.8	26.6

[a] Gas-phase QM calculations corrected for solvent effects using the PDDG/PM3/MM/FEP simulations.

[b] Ref 3.

Table 7

Solution-Phase Free Energy Activation Barriers, $\Delta G^{\ddagger}$ (kcal/mol), for the Menshutkin Reaction Between Triethylamine and Ethyl Iodide Using B3LYP and Mixed Basis Sets.[a]

C, H, N	I	THF-POL	CCl_4-POL	Cyclohex-POL
6-31+G(d,p)	aug-cc-PVTZ-PP	31.2	41.1	37.3
6-31+G(d,p)	SDB-aug-cc-PVTZ	31.0	40.9	37.1
aug-cc-PVDZ	aug-cc-PVTZ-PP	26.4	36.3	32.5
aug-cc-PVDZ	SDB-aug-cc-PVTZ	26.1	36.0	32.2

[a]Gas-phase QM calculations corrected for solvent effects using the PDDG/PM3/MM/FEPsimulations.

Table 8

Mean Absolute Errors (MAE) in $\Delta G^{\ddagger}$ (kcal/mol) for the Solution-Phase Menshutkin Reactions.

	OPLS	OPLS-AAP [a]
B3LYP/LANL2DZ	5.4	3.4
B3LYP/LANL2DZd	5.2	3.2
B3LYP/SVP	7.6	6.1
B3LYP/MIDI!	4.9	3.1
B3LYP/6-311G(d,p)	5.8	4.3
MP2/LANL2DZ	5.4	3.3
MP2/LANL2DZd	7.0	5.8
PDDG/PM3	5.3	3.8

[a] Polarized OPLS-AAP force field for THF, CCl_4 and cyclohexane only, all other solvents used the non-polarized OPLS.

Table 9

Mean Absolute Errors (MAE) in $\Delta G^{\ddagger}$ (kcal/mol) for the Solution-Phase Menshutkin Reactions Using Mixed Basis Sets.[a]

C, H, N	I	OPLS	OPLS-AAP [a]
6-31+G(d,p)	aug-cc-PVTZ-PP	10.3	8.8
6-31+G(d,p)	SDB-aug-cc-PVTZ	10.1	8.6
aug-cc-PVDZ	aug-cc-PVTZ-PP	6.3	4.8
aug-cc-PVDZ	SDB-aug-cc-PVTZ	6.1	4.6

[a] Polarized OPLS-AAP force field for THF, CCl_4 and cyclohexane only, all other solvents used the non-polarized OPLS.